Electronic Supplementary Information (ESI)

Transmetalated synthesis of homodinuclear Mn^{II} and Co^{II} complexes containing Robson type macrocyclic ligands: crystal structure, magnetic investigation and DFT calculations

Abhishek Pramanik, Samit Majumder, Susanta Hazra and Sasankasekhar Mohanta*

Department of Chemistry, University of Calcutta, 92 A. P. C. Road, Kolkata 700009, India, E-mail: sm_cu_chem@yahoo.co.in; smchem@caluniv.ac.in.

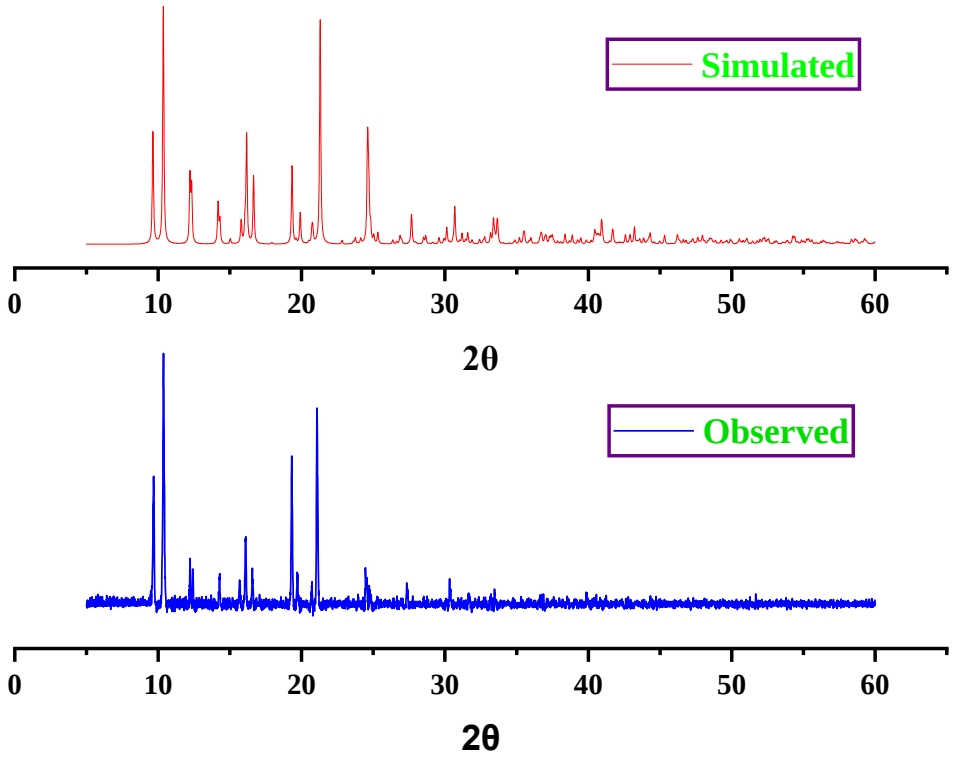

Fig. S1. Powder X-ray diffraction (PXRD) patterns of $[Mn^{II}_2L^1Cl_2]$ (**1**).

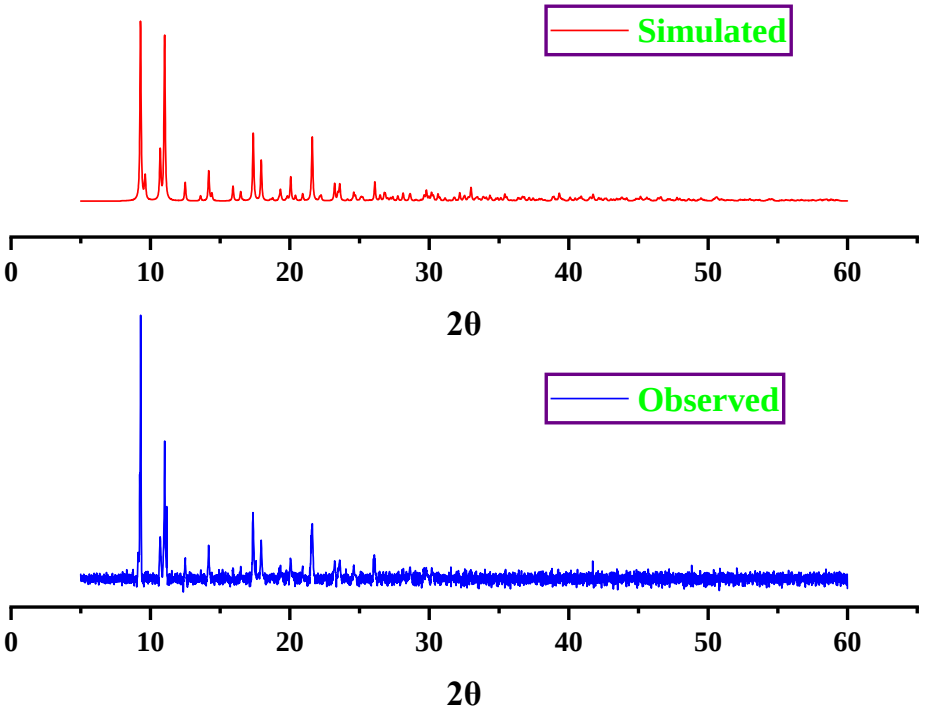

Fig. S2. Powder X-ray diffraction (PXRD) patterns of $[Co^{II}_2L^2(CH_3OH)(H_2O)Cl](NO_3)$ (**2**).

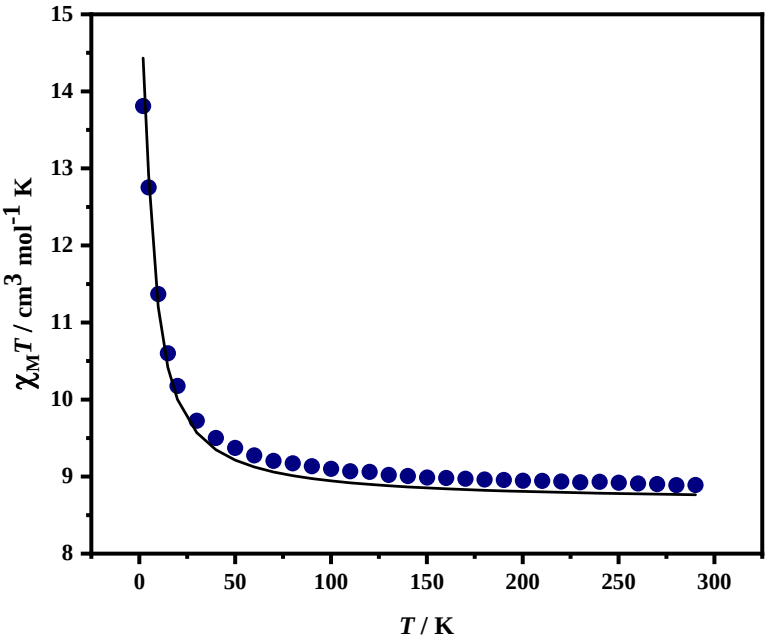

Fig. S3. $\chi_M T$ versus T plot (at 0.1 T) for $[Mn^{II}_2L^1Cl_2]$ (**1**). Symbols represent the experimental data while the solid line represents the simulated profile having J = 0.377 cm^{-1}, g = 1.990 and residual (R) = 2.09 × 10^{-1}.

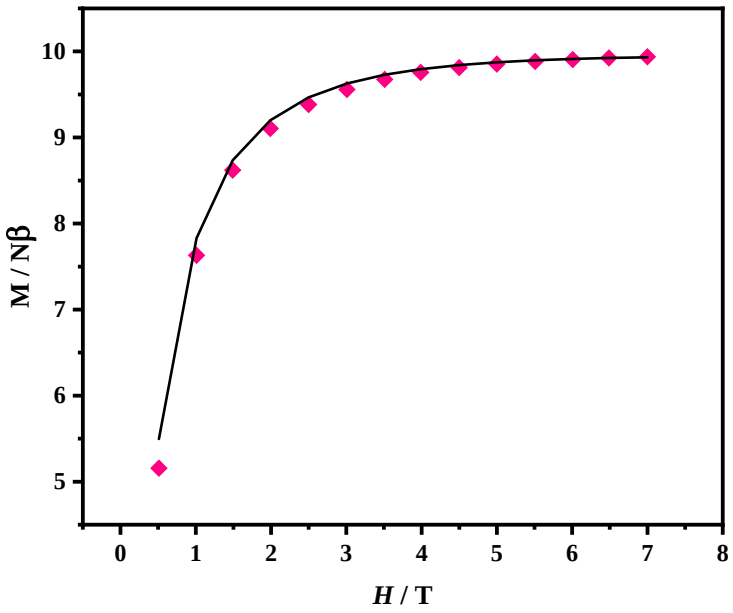

Fig. S4. Magnetization versus field plot (at 2 K) for $[Mn^{II}_2L^1Cl_2]$ (**1**). Symbols represent the experimental data while the solid line represents the simulated profile having J = 0.377 cm^{-1}, g = 1.990 and residual (R) = 2.09 × 10^{-1}.

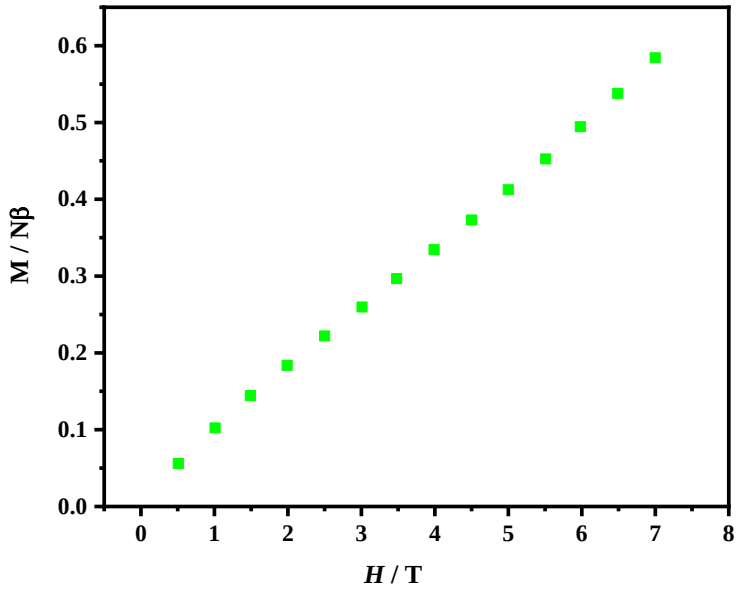

Fig. S5. Experimental magnetization versus field plot (at 2 K) for $[Co^{II}_2L^2(CH_3OH)(H_2O)Cl](NO_3)$ (**2**).

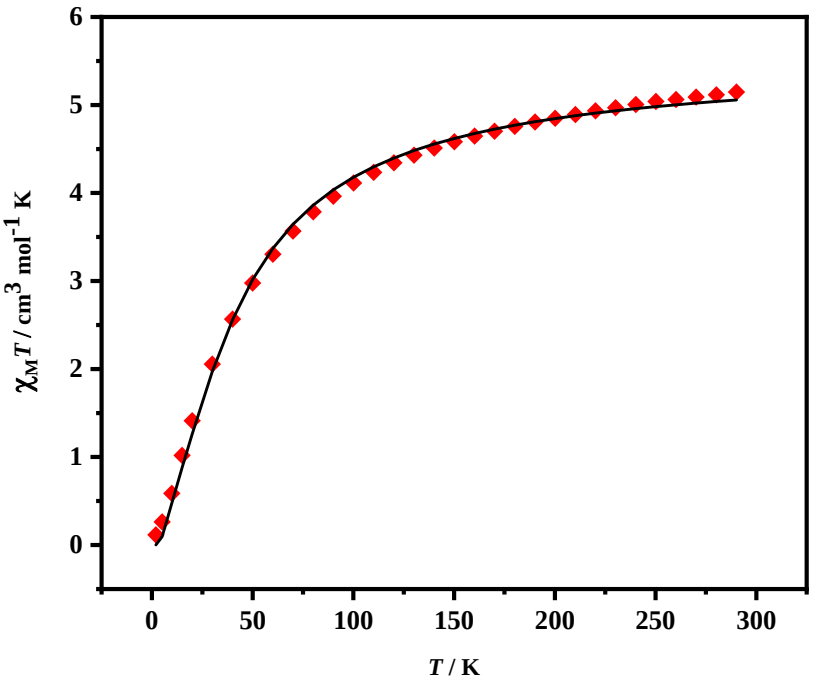

Fig. S6. $\chi_M T$ versus T plot (at 1 T) for $[Co^{II}_2L^2(CH_3OH)(H_2O)Cl](NO_3)$ (**2**). Symbols represent the experimental data while the solid line represents the simulated profile having J = –6.74 cm^{-1}, g = 2.427 and residual (R) = 1.75×10^{-1}.

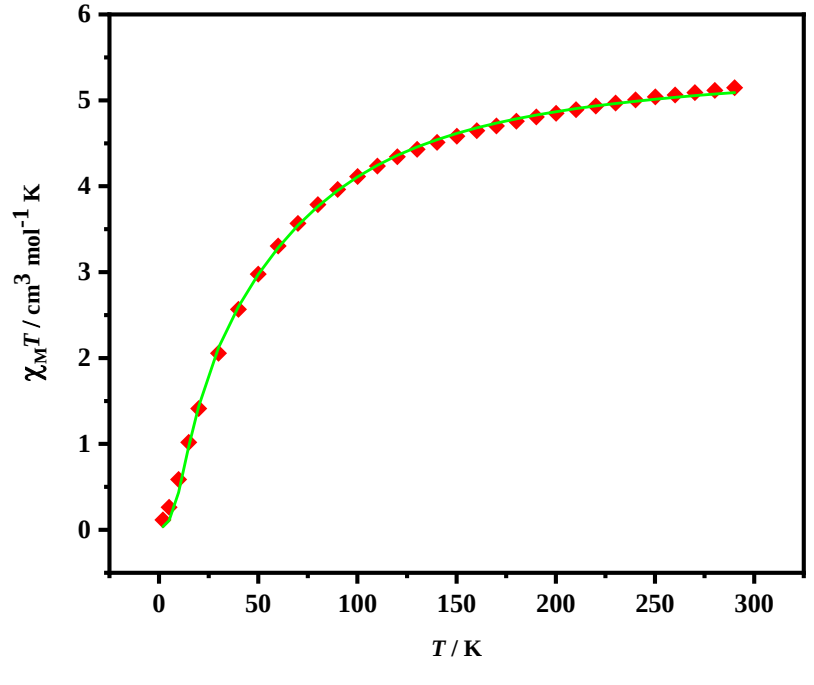

Fig. S7. $\chi_M T$ versus T plot (at 1 T) for $[Co^{II}_2L^2(CH_3OH)(H_2O)Cl](NO_3)$ (**2**). Symbols represent the experimental data while the solid line represents the simulated profile having J = –4.5 cm^{-1}, g = 2.417, D = 69.5 cm^{-1} and residual (R) = 7.76×10^{-2}.

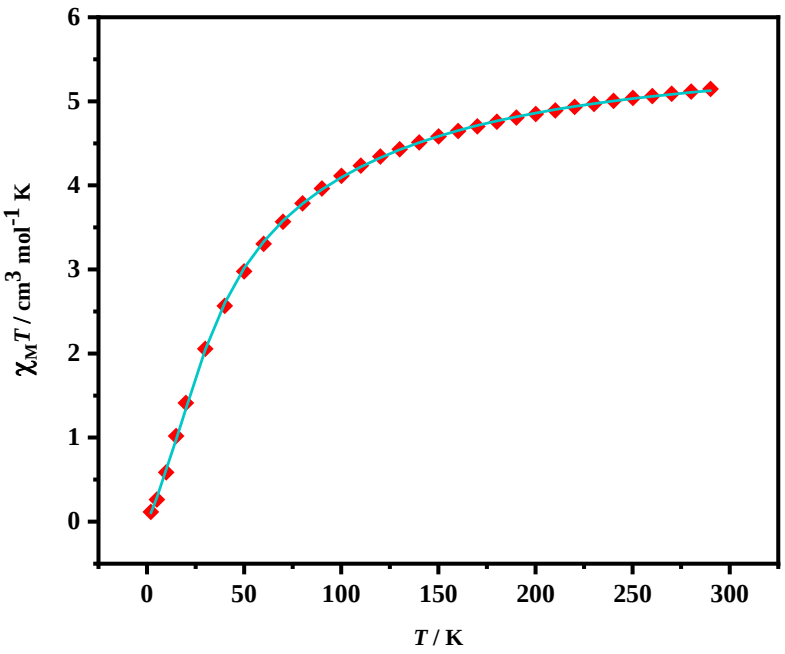

Fig. S8. $\chi_M T$ versus T plot (at 1 T) for $[Co^{II}_2L^2(CH_3OH)(H_2O)Cl](NO_3)$ (**2**). Symbols represent the experimental data while the solid line represents the simulated profile having J = –5.9 cm^{-1}, g = 2.454, D_1 = 121.6 cm^{-1}, D_2 = 11.1 cm^{-1} and residual (R) = 1.45 × 10^{-2}.

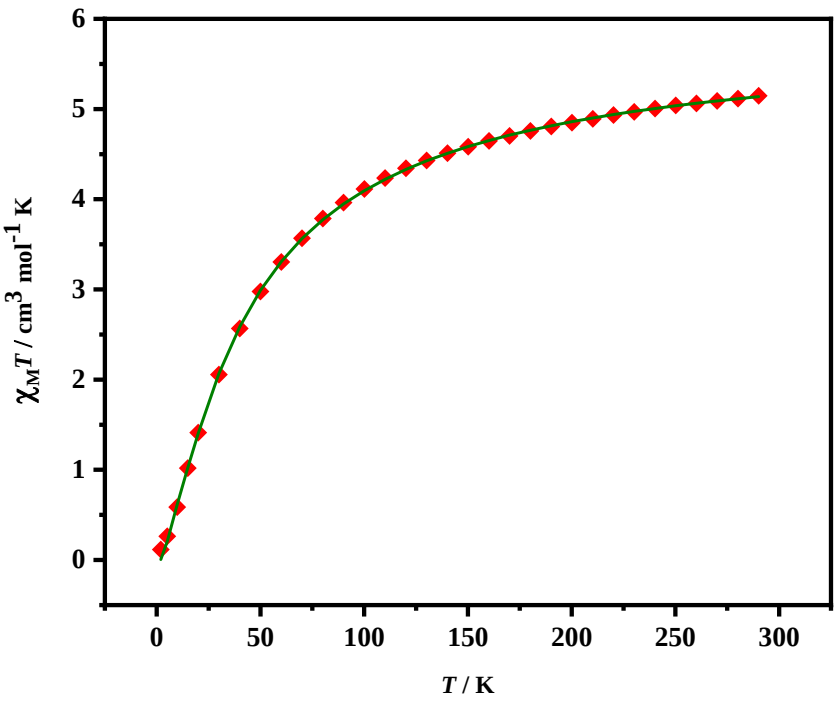

Fig. S9. $\chi_M T$ versus T plot (at 1 T) for $[Co^{II}_2L^2(CH_3OH)(H_2O)Cl](NO_3)$ (**2**). Symbols represent the experimental data while the solid line represents the simulated profile having J = –5.04 cm^{-1}, g = 2.496, zJ' = –0.90 cm^{-1} and residual (R) = 1.87 × 10^{-2}.

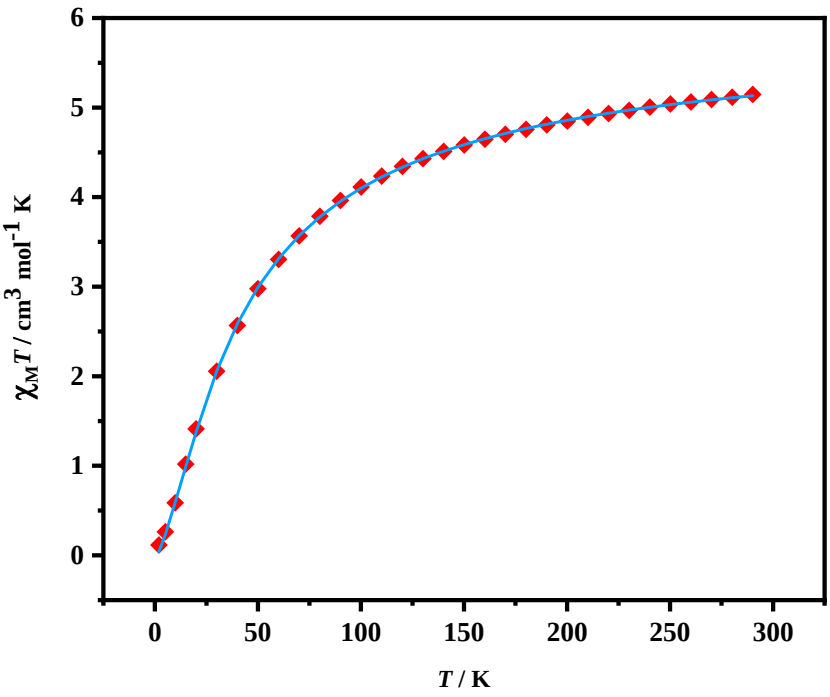

Fig. S10. $\chi_M T$ versus T plot (at 1 T) for $[Co^{II}_2L^2(CH_3OH)(H_2O)Cl](NO_3)$ (**2**). Symbols represent the experimental data while the solid line represents the simulated profile having $J = -4.0$ cm^{-1}, g = 2.495, $D = 18.9$ cm^{-1}, $zJ' = -1.077$ cm^{-1} and residual (R) = 5.30×10^{-3}.

HS	BS
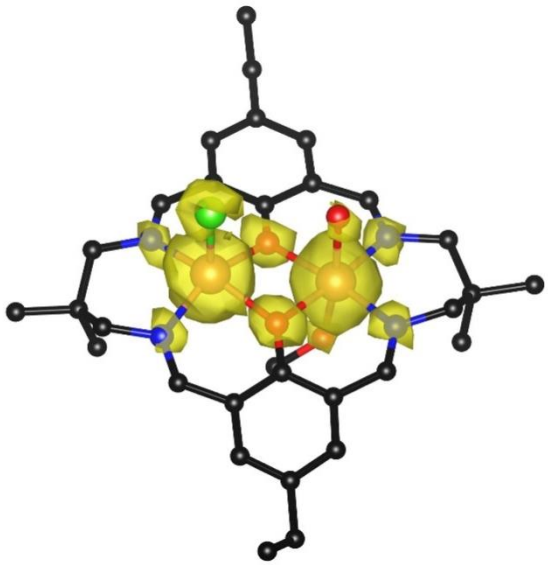	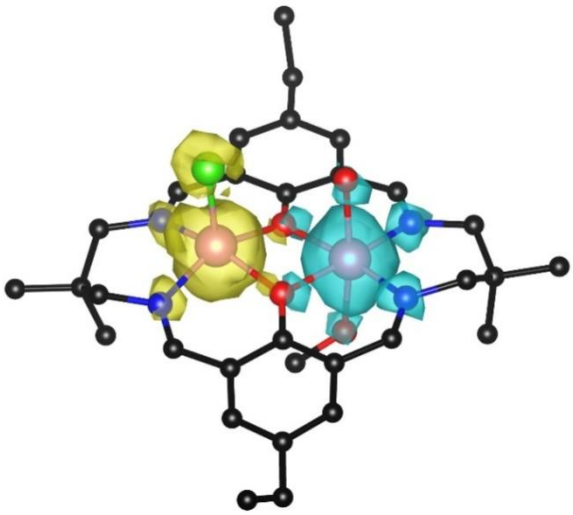
High spin state	**Broken symmetry state**

Fig. S11. DFT computed spin densities (iso = 0.003) of $[Co^{II}_2L^2(CH_3OH)(H_2O)Cl](NO_3)$ (**2**) in two spin states (HS and BS).

Table S1. Selected bond lengths (in Å) and bond angles (in ˚) in the single crystal structure of $[Mn^{II}_2L^1Cl_2]$ (**1**).

Mn1–O1	2.1292
Mn1–O1A	2.1025
Mn1–N1	2.1655
Mn1–N2	2.1872
Mn1–Cl1	2.3437
Mn1–Mn1A	3.307
O1–Mn1–N2	141.09
O1A–Mn1–N1	145.02
O1A–Mn1–O1	77.22
O1A–Mn1–N2	85.00
N2–Mn1–N1	91.73
O1–Mn1–N1	84.02
Cl1–Mn1–O1	111.74
Cl1–Mn1–O1A	113.79
Cl1–Mn1–N1	100.49
Cl1–Mn1–N2	107.07
Mn1– O1–Mn1A	102.78

Table S2. Selected bond lengths (in Å) and bond angles (in °) in the single crystal structure of $[Co^{II}_2L^2(CH_3OH)(H_2O)Cl](NO_3)$ (**2**).

Co1–O1	2.052
Co1–O2	2.044
Co1–N1	2.042
Co1–N2	2.072
Co1–Cl1	2.295
Co2–O1	2.037
Co2–O2	2.021
Co2–N3	2.047
Co2–N4	2.028
Co2–O3	2.179
Co2–O4	2.214
Co1–Co2	3.131
O1–Co1–N2	154.6
O2–Co1–N1	151.3
O1–Co1–N1	87.95
N2–Co1–N1	95.2
N2–Co1–O2	87.40
O1–Co1–O2	78.20
Cl1–Co1–O1	103.00
Cl1–Co1–O2	103.30
Cl1–Co1–N1	104.29
Cl1–Co1–N2	100.63
N4–Co2–O2	169.87
N3–Co2–O1	172.98
O3–Co2–O4	170.6
N3–Co2–N4	95.73
N4–Co2–O1	90.90
O1–Co2–O2	79.08
N3–Co2–O2	94.34
N3–Co2–O3	89.5
N4–Co2–O3	93.85
O1–Co2–O3	92.37
O2–Co2–O3	85.13
N3–Co2–O4	88.93
N4–Co2–O4	95.5
O1–Co2–O4	88.14
O2–Co2–O4	85.77
Co1– O1–Co2	99.95
Co1– O2–Co2	100.72

Table S3. The values of the simulated magnetic parameters for $[Co^{II}_2L^2(CH_3OH)(H_2O)Cl](NO_3)$ (**2**) obtained by taking into account *J* and *g*.

Sl. No.	***J* (cm^{-1})**	***g***	**Residual (*R*)**
I	–6.74	2.427	1.75×10^{-1}

Table S4. The values of the simulated magnetic parameters for $[Co^{II}_2L^2(CH_3OH)(H_2O)Cl](NO_3)$ (**2**) obtained by taking into account *J*, *g* and an average *D* for the two Co^{II} centres.

Sl. No.	***J* (cm^{-1})**	***g***	***D* (cm^{-1})**	**Residual (*R*)**
I	−4.0	2.417	83.4	1.54×10^{-1}
II	−4.2	2.418	78.2	1.01×10^{-1}
III	−4.3	2.418	75.4	8.68×10^{-2}
IV	−4.4	2.418	72.5	7.92×10^{-2}
V	−4.5	2.417	69.5	7.76×10^{-2}
VI	−4.6	2.417	66.4	8.12×10^{-2}
VII	−4.7	2.416	63.2	8.93×10^{-2}
VIII	−5.0	2.414	53.4	1.33×10^{-1}
IX	−5.5	2.411	36.5	2.22×10^{-1}
X	−6.0	2.409	17.9	2.64×10^{-1}
XI	−6.5	2.418	4.2	1.90×10^{-1}
XII	−6.7	2.425	0.003	1.75×10^{-1}
XIII	−7.0	2.436	0.0002	1.94×10^{-1}

Table S5. The values of the simulated magnetic parameters for $[Co^{II}_2L^2(CH_3OH)(H_2O)Cl](NO_3)$ (**2**) obtained by taking into account *J*, *g* and two distinct *D* for the two Co^{II} centres.

Sl. No.	***J* (cm^{-1})**	***g***	***D*$_1$ (cm^{-1})**	***D*$_2$ (cm^{-1})**	**Residual**
I	−4.0	2.417	83.4	83.4	1.54×10^{-1}
II	−4.5	2.426	104.4	50.0	7.12×10^{-2}
III	−5.0	2.440	126.8	28.2	5.58×10^{-2}
IV	−5.8	2.453	123.3	12.1	1.57×10^{-2}
V	−5.9	2.454	121.6	11.1	1.45×10^{-2}
VI	−6.0	2.456	119.4	10.3	1.62×10^{-2}
VII	−6.4	2.453	93.2	7.2	4.42×10^{-2}
VIII	−6.7	2.423	7.7	−6.1	1.06×10^{-1}
IX	−7.0	2.454	−65.2	−0.45	2.59×10^{-2}
X	−7.1	2.453	−56.9	0.06	3.14×10^{-2}

Table S6. The values of the simulated magnetic parameters for $[Co^{II}_2L^2(CH_3OH)(H_2O)Cl](NO_3)$ (**2**) obtained by taking into account *J*, *g* and *zJ′*.

Sl. No.	J (cm^{-1})	g	zJ' (cm^{-1})	Residual (R)
I	−4.0	2.523	−1.31	6.30×10^{-2}
II	−4.5	2.510	−1.121	3.15×10^{-2}
III	−5.0	2.497	−0.92	1.88×10^{-2}
IV	−5.04	2.496	−0.90	1.87×10^{-2}
V	−5.1	2.494	−0.88	1.88×10^{-2}
VI	−5.5	2.483	−0.72	2.76×10^{-2}
VII	−6.0	2.469	−0.49	5.90×10^{-2}

Table S7. The values of the simulated magnetic parameters for $[Co^{II}_2L^2(CH_3OH)(H_2O)Cl](NO_3)$ (**2**) obtained by taking into account *J*, *g*, an average *D* for the two Co^{II} centres, and *zJ′*

Sl. No.	J (cm^{-1})	g	D (cm^{-1})	zJ' (cm^{-1})	Residual (R)
I	−3.5	2.498	25.3	−1.170	1.33×10^{-2}
II	−3.9	2.494	20.9	−1.083	5.36×10^{-3}
III	−4.0	2.495	18.9	−1.077	5.30×10^{-3}
IV	−4.1	2.496	16.8	−1.072	5.57×10^{-3}
V	−4.5	2.498	10.1	−1.023	6.79×10^{-3}
VI	−5.0	2.492	5.8	−883	1.06×10^{-2}

Table S8. The values of the simulated magnetic parameters for $[Co^{II}_2L^2(CH_3OH)(H_2O)Cl](NO_3)$ (**2**) obtained by taking into account *J*, *g*, distinct *D* for the two Co^{II} centres, and *zJ′*

Sl. No.	J (cm^{-1})	g	D_1 (cm^{-1})	D_2 (cm^{-1})	zJ' (cm^{-1})	Residual
I	−3.5	2.498	25.2	25.2	−1.17	1.29×10^{-2}
II	−3.8	2.494	22.4	22.4	−1.09	5.91×10^{-3}
III	−4.0	2.494	−38.3	−6.0	−1.05	4.92×10^{-3}
IV	−4.3	2.484	37.8	11.9	−0.91	4.11×10^{-3}
V	−4.5	2.498	−17.4	−4.1	−1.02	5.28×10^{-3}
VI	−5.0	2.491	13.4	3.4	−0.87	7.16×10^{-3}
VII	−5.5	2.480	15.9	1.5	−0.68	1.23×10^{-2}

Table S9. Continuous Shape measures calculation for $[Mn^{II}_2L^1Cl_2]$ (**1**) and $[Co^{II}_2L^2(CH_3OH)(H_2O)Cl](NO_3)$ (**2**) obtained using SHAPE.

Compound	**Metal Centre**	Coordination Number	Pentagon (D_{5h})	Vacant octahedron (C_{4v})	Trigonal bipyramid (D_{3h})	Spherical square pyramid (C_{4v})	Johnson trigonal bipyramid J12(D_{3h})
1	Mn	5	29.869	4.007	5.236	**0.866**	9.191
2	Co1	5	31.437	2.453	5.031	**0.436**	8.285
		Coordination Number	Hexagon (D6h)	Pentagonal pyramid (C5v)	Octahedron (Oh)	Trigonal prism (D3h)	Johnson pentagonal pyramid J2 (C5v)
	Co2	6	32.412	26.360	**0.557**	14.179	30.280

Table S10. The geometries of the hydrogen bonds in the supramolecular topologies of $[Mn^{II}_2L^1Cl_2]$ (**1**) and $[Co^{II}_2L^2(CH_3OH)(H_2O)Cl](NO_3)$ (**2**) (distances in Å and angles are in °). Symmetry in **1**: C, 2–x, 0.5+y, 0.5–z. Symmetry in **2**: *E*, –0.5+x, 1.5–y, z.

	D–H···A	D···A	H···A	D–H···A
1	C5–H5···Cl1C	3.580	2.788	146.03
	C8–H8···Cl1C	3.662	2.824	139.76
2	C30–H30A···O7E	3.429	2.489	158.60
	C31–H31C···O7	3.170	2.388	136.38
	O4–H4···O7	3.295	2.613	134.97
	O4–H4···O5	2.771	1.894	173.74
	O3–H3A···O6E	2.801	2.000	152.41
	O3–H3B···Cl1	3.218	2.428	151.13

Table S11. Shortest intermolecular metal–metal separations (in Å) in $[Mn^{II}_2L^1Cl_2]$ (**1**) and $[Co^{II}_2L^2(CH_3OH)(H_2O)Cl](NO_3)$ (**2**). Atom labels correspond to the contacts, shown in Figs. 2 and 3 in main text.

1		**2**	
Mn1-------Mn1B	8.650	Co1-----Co1D	13.051
Mn1-------Mn1E	10.266	Co1-----Co2D	10.836
Mn1A-----Mn1B	7.678	Co2-----Co1D	12.150
Mn1A-----Mn1E	9.790	Co2-----Co2D	10.072

Table S12: Crystallographic Data for **1** and **2**.

Compound	**1**	**2**
Empirical formula	$C_{28}H_{34}N_4O_2Cl_2Mn_2$	$C_{31}H_{44}N_5O_7ClCo_2$
Formula weight	639.37	752.02
Crystal system	monoclinic	Orthorhombic
Space group	*P2(1)/c*	*Pna21*
a (Å)	9.7907(6)	18.357(10)
b (Å)	11.7780(7)	11.122(5)
c (Å)	13.2080(8)	16.532(7)
α (°)	90.00	90
β (°)	110.505(2)	90
γ (°)	90.00	90
V (Å^3)	1426.58(15)	3375(3)
Z	2	4
D (calculated, g cm^{-3})	1.488	1.480
λ (Mo K$_\alpha$), Å	0.71073	0.71073
μ(mm^{-1})	1.105	1.115
T (K)	296(2)	160(2)
F(000)	660	1568
2θ range for data collection (°)	4.44–54.90	4.414–59.232
Index ranges	$-12 \le h \le 11$	$-25 \le h \le 25$
	$-15 \le k \le 15$	$-15 \le k \le 15$
	$-17 \le l \le 16$	$-16 \le l \le 22$
No. measured reflections	19174	44280
No. independent reflections	3219	7996
R_{int}	0.0463	0.0882
No. refined parameters	240	426
No. observed reflections, $I \ge 2\sigma(I)$	2556	6409
R_1[a], wR_2[b] [$I \ge 2\sigma(I)$]	0.03096, 0.0668	0.0505, 0.1281
R_1[a], wR_2[b] [all data]	0.0466, 0.0725	0.0755, 0.1570

$^aR_1 = [\sum||F_o|-|F_c||/\sum|F_o|]$. $^bwR_2 = [\sum w(F_o^2-F_c^2)^2/\sum w(F_o^2)^2]^{1/2}$